MAGNETOHYDRODYNAMIC FLOW AND HEAT TRANSFER OF A JEFFREY FLUID TOWARDS A STRETCHING VERTICAL SURFACE

by

Kartini AHMAD[a*] and Anuar ISHAK[b]

[a] Department of Science in Engineering, Kulliyyah of Engineering, International Islamic University, Kuala Lumpur, Malaysia
[b] School of Mathematical Sciences, Faculty of Science and Technology, Universiti Kebangsaan Malaysia, Selangor, Malaysia

Original scientific paper
DOI:10.2298/TSCI141103029A

This study investigates the steady-mixed convection boundary layer flow near a stagnation point that runs about a linearly stretched vertical surface filled with a Jeffery fluid in the presence of a transverse magnetic field. It is assumed that the external velocity impinges normally to the wall and the wall temperature varies linearly with the distance from the stagnation point. The governing partial differential equations that govern the fluid flow are transformed into a set of coupled ordinary differential equations, which are then solved numerically using a finite difference scheme. The numerical results are presented for some values of parameters, namely Deborah number, Prandtl number, magnetic parameter, and the mixed convection parameter, for both assisting and opposing flows.

Key words: *stagnation flow, Jeffrey fluid, heat transfer, boundary layer, fluid dynamics*

Introduction

Industrially, the process for stretching sheet has significant relevance to several practical applications, such as the extrusion of metals, plastics and polymers, *etc.* During the rubber and plastic sheets manufacturing process, a gaseous medium, through the not-yet solidified material, is blown. As such, the study of heat transfer and flow field is necessary to determine the quality of the final products, as explained by Karwe and Jaluria [1]. It seems that Crane [2] was the first to give a similarity solution in closed analytical form for steady 2-D incompressible boundary layer flow caused by the stretching of a sheet, which moves in its own plane with a velocity varying linearly with distance from a fixed point. Flow which moves towards a vertical surface will create a flow with buoyancy force due to the existence of the temperature difference between the wall and the free stream. Such flow is known as the mixed convection flow. Hiemenz [3] was the first to investigate the 2-D stagnation flow towards a stationary semi-infinite wall by using similarity transformation in order to reduce the Navier-Stokes equation to a non-linear ordinary differential equation. Since then, lots of research have been carried out to investigate the mixed convection flow towards a vertical sheet, [4-9]. It is worth mentioning that the work of Ishak *et al*. [4] has been extended by Saleh *et al*. [10] to the case of a shrinking sheet. A study on the mixed convection boundary layer flow over a vertical permeable cylinder

* Corresponding author, e-mail: kartini@iium.edu.my

has been conducted by Ellahi *et al*. [11]. On the other hand, MHD flow and heat transfer has been studied in [12-14].

In all previously mentioned papers, however, investigators confine their studies to Newtonian fluid flow problems, which is inadequate to describe some fluid properties. As such, non-Newtonian fluids, which exhibit a non-linear relationship between the stresses and the rate of strains, are found to be more interesting than Newtonian fluids. There are numerous references on the stagnation point flow towards a vertical surface in various types of non-Newtonian fluids, which can be found in the literature, and some of them can be found in [15-19]. The MHD flow of a non-Newtonian fluid was considered in [20-27].

The aim of the present study is to extend the work done by Ishak *et al*. [4], by investigating the flow of one kind of Oldroyd model, *i. e.* Jeffery's version, which impinges normally on a heated or cooled vertical surface that is being stretched. This fluid model includes elastic and memory effects exhibited by dilute polymer solutions and biological fluids, Hayat *et al*. [28]. Even though the literature on the Jeffery fluid flow is scarce, the fluid is one of great importance. Quite recently, the flow of a Jeffrey fluid in eccentric cylinders was investigated by Ellahi *et al*. [21].

Problem formulation

Consider a steady 2-D laminar boundary layer stagnation-point flow of an incompressible electrically-conducting Jeffery's fluid, impinging normally towards a vertical surface. It is assumed that the ambient fluid moves with velocity $u_e(x) = ax$ in the y-direction towards the stagnation point on the plate, with the temperature varying linearly along it with $T_w(x) = T_\infty + bx$, where a (> 0) and b are arbitrary constants. The continuous stretching plate is assumed to have a velocity of the form $u_w(x) = cx$, where $c > 0$ is a constant.

Assume that a uniform magnetic field of strength, B_0, is applied in the positive y-direction normal to the plate, and the induced magnetic field due to the magnetic Reynolds number is taken to be small enough and assumed to be negligible in comparison to the applied magnetic field. Under these assumptions, along with the Boussinesq and boundary layer approximations, the basic equations of the problem can be written:

$$\frac{\partial u}{\partial x} + \frac{\partial v}{\partial y} = 0 \tag{1}$$

$$u\frac{\partial u}{\partial x} + v\frac{\partial v}{\partial y} = u_e\frac{\mathrm{d}u_e}{\mathrm{d}x} + \frac{\nu}{1+\lambda_1}\left[\frac{\partial^2 u}{\partial y^2} + \lambda_2\left(u\frac{\partial^3 u}{\partial x \partial y^2} - \frac{\partial u}{\partial x}\frac{\partial^2 u}{\partial y^2} + \frac{\partial u}{\partial y}\frac{\partial^2 u}{\partial x \partial y} + v\frac{\partial^3 u}{\partial y^3}\right)\right] + \frac{\sigma B_o^{\,2}}{\rho}\left(u_e - u\right) \pm \mathrm{g}\beta\left(T - T_\infty\right) \tag{2}$$

$$u\frac{\partial T}{\partial x} + v\frac{\partial T}{\partial y} = \alpha\frac{\partial^2 T}{\partial y^2} \tag{3}$$

subject to the boundary conditions:

$$\begin{aligned} &u = u_w(x), \quad v = 0, \qquad T = T_w \quad \text{at} \quad y = 0 \\ &u \to u_e(x), \quad \frac{\partial u}{\partial y} \to 0, \quad T \to T_\infty \quad \text{as} \quad y \to \infty \end{aligned} \tag{4}$$

where u and v are the velocity components along the x- and y-axes, respectively, g – the acceleration due to the gravity, and T – the fluid temperature in the boundary layer. Further, ν, λ_1, λ_2, ρ, β, and α are, respectively, the kinematic viscosity, ratio of the relaxation and retardation times, relaxation time, fluid density, thermal expansion coefficient, and thermal diffusivity. The ± sign in the last term of eq. (2) represents the influence of the thermal buoyancy force, with "+" and "–" signs pertaining to the buoyancy assisting and opposing flow regions, respectively. According to Ramachandran *et al*. [29], the assisting flow exists if the upper half of the flat plate is heated while the lower half of the plate is cooled. In this case, the flow near the heated flat surface tends to move upward, and the flow near the cooled flat plate tends to move downward. Therefore, this behaviour acts to assist the flow field. The reverse trend can be observed in the opposing flow.

We look at the solutions of eqs. (1)-(3) in the following forms:

$$\psi = \sqrt{\nu x u_w}\, f(\eta), \quad \theta(\eta) = \frac{T - T_\infty}{T_w - T_\infty}, \quad \eta = \sqrt{\frac{u_w}{\nu x}}\, y \tag{5}$$

where ψ is the stream function, it is defined in the usual way as $u = \partial\psi/\partial y$ and $v = -\partial\psi/\partial x$. Thus, we have:

$$u = c\, x\, f'(\eta), \quad v = -\sqrt{c\nu}\, f(\eta) \tag{6}$$

where prime denotes differentiation with respect to η. Substituting variables (5) and (6) into eqs. (1)-(3), eq. (1) is automatically satisfied and eqs. (2) and (3) are reduced to:

$$f''' + \gamma\left(f''^2 - ff^{iv}\right) + \left(1 + \lambda_1\right)\left[\frac{a^2}{c^2} \pm \lambda\theta + M\left(1 - f'\right) - f'^2 + ff''\right] = 0 \tag{7}$$

$$\theta'' + \mathrm{Pr}\left(f\theta' - f'\theta\right) = 0 \tag{8}$$

and the transformed boundary conditions can be written:

$$\begin{gathered} f(0) = 0, \quad f'(0) = 1, \quad \theta(0) = 1, \quad \text{at} \quad \eta = 0 \\ f'(\eta) \to \frac{a}{c}, \quad f''(\eta) \to 0, \quad \theta(\eta) \to 0 \quad \text{as} \quad \eta \to \infty \end{gathered} \tag{9}$$

Here, $\gamma = c\lambda_2$ is the Deborah number, $M = a\sigma B_0^2/(\rho c^2)$ – the MHD parameter, $\mathrm{Pr} = \nu/\alpha$ – the Prandtl number, and $\lambda = \mathrm{Gr}_x/\mathrm{Re}_x^2$ – the mixed convection parameter where $\mathrm{Gr}_x = g\beta(T_w - T_\infty)x^3/\nu^2$ is the local Grashof number and $\mathrm{Re}_x = u_w x/\nu$ is the local Reynolds number. We note that λ is a constant, with $\lambda > 0$ and $\lambda < 0$ corresponding to the opposing and assisting flows, respectively, while $\lambda = 0$ (*i. e.* $T_w = T_\infty$) for pure forced convection flow. It should be pointed out that for $\gamma = \lambda_1 = M = 0$, the problem is reduced to that of Ishak *et al.* [4].

The physical quantities of principle interest are the skin friction coefficient, C_f, and the local Nusselt number, Nu_x, which are defined:

$$C_f = \frac{\tau_w}{\dfrac{\rho u_e^{\,2}}{2}}, \quad \mathrm{Nu}_x = \frac{x q_w}{k(T_w - T_\infty)} \tag{10}$$

where τ_w and q_w are the wall shear stress and the heat flux from the surface, respectively, which are given by:

$$\tau_w = \mu\left(\frac{\partial u}{\partial y}\right)_{y=0}, \quad q_w = -k\left(\frac{\partial T}{\partial y}\right)_{y=0} \tag{11}$$

where μ and k being the dynamic viscosity and the thermal conductivity, respectively. Substituting eqs. (5) and (6) into eq. (9), the scaled skin friction coefficient and the local Nusselt number reduce to:

$$C_f\sqrt{\mathrm{Re}_x} = f''(0), \quad \frac{\mathrm{Nu}_x}{\sqrt{\mathrm{Re}_x}} = -\theta'(0) \tag{12}$$

where $\mathrm{Re}_x = u_w x/\nu$ is the local Reynolds number.

Results and discussions

The ordinary differential eqs. (7) and (8), subject to the boundary conditions (9), have been solved numerically using the Keller-box method for some values of the governing parameters, *i. e.* the magnetic parameter, M, the material parameter (Deborah number), γ, the mixed convection parameter, λ, the Prandtl number, and the velocity ratio of a/c. The detailed procedure of this method can be found in the books by Cebeci [30] and Cebeci and Bradshaw [31].

In order to validate the present code, the present results obtained for the skin friction coefficient $C_f(\mathrm{Re}_x)^{1/2}$ when $\gamma = M = \lambda = 0$ for several values of a/c are compared with Ishak *et al*. [4], Mahapatra and Gupta [32], and Nazar *et al*. [33] and as shown in tab. 1, whereas the present values obtained for the $C_f(\mathrm{Re}_x)^{1/2}$ and the $\mathrm{Nu}_x(\mathrm{Re}_x)^{-1/2}$ for different values of Prandtl number when $M = \gamma = 0$ and $\lambda = a/c = 1$, for both assisting and opposing flows, are compared with Ishak *et al*. [4] as tabulated in tab. 2, along with the new results obtained for the $C_f(\mathrm{Re}_x)^{1/2}$ and the $\mathrm{Nu}_x(\mathrm{Re}_x)^{-1/2}$ for various values of the Deborah number. For the sake of brevity, the following results of this paper are limited to $\lambda_1 = 0$. It can be seen from tabs. 1 and 2, the values of $C_f(\mathrm{Re}_x)^{1/2}$ and $\mathrm{Nu}_x(\mathrm{Re}_x)^{-1/2}$ obtained are found to be in a good agreement with previously published results, thus gives great confident to the numerical code used in the present study.

Table 1. Comparisons of $C_f(\mathrm{Re}_x)^{1/2}$ values obtained when $\gamma = M = \lambda = 0$ for some values of a/c

a/c	Mahapatra and Gupta [32]	Nazar *et al*. [33]	Ishak *et al*. [4]	Present results
0.1	–0.9694	–0.9694	–0.9694	–0.9694
0.2	–0.9181	–0.9181	–0.9181	–0.9181
0.5	–0.6673	–0.6673	–0.6673	–0.6673
2	2.0175	2.0176	2.0175	2.0175
3	4.7293	4.7296	4.7294	4.7293

Table 2. Values of $C_f(\mathrm{Re}_x)^{1/2}$ and $\mathrm{Nu}_x(\mathrm{Re}_x)^{-1/2}$ obtained for various γ and Prandtl number when $M = 0$ and $\lambda = a/c = 1$; results in ( ) are those of Ishak *et al*. [4]

γ	Pr	Buoyancy assisting flow		Buoyancy opposing flow	
		$C_f(\mathrm{Re}_x)^{1/2}$	$\mathrm{Nu}_x(\mathrm{Re}_x)^{-1/2}$	$C_f(\mathrm{Re}_x)^{1/2}$	$\mathrm{Nu}_x(\mathrm{Re}_x)^{-1/2}$
0	0.72	0.3645 (0.3645)	1.0931 (1.0931)	–0.3852 (–0.3852)	1.0292 (1.0293)
	6.8	0.1804 (0.1804)	3.2901 (3.2902)	–0.1832 (–0.1832)	3.2465 (3.2466)
	20	0.1175 (0.1175)	5.6229 (5.6230)	–0.1183 (–0.1183)	5.5921 (5.5923)
1	0.72	0.2355	1.0806	–0.2419	1.0445
	6.8	0.1091	3.2782	–0.1026	3.2581
	20	0.0635	5.6127	–0.0637	5.5991
2	0.72	0.1719	1.0759	–0.1754	1.0501
	6.8	0.0705	3.2747	–0.0708	3.2619
	20	0.0433	5.6104	–0.0434	5.6011

Various cases are plotted for the skin friction coefficient and the local Nusselt number for assisting and opposing flows, as shown in figs. 1-3. The effect of the Deborah number is illus-

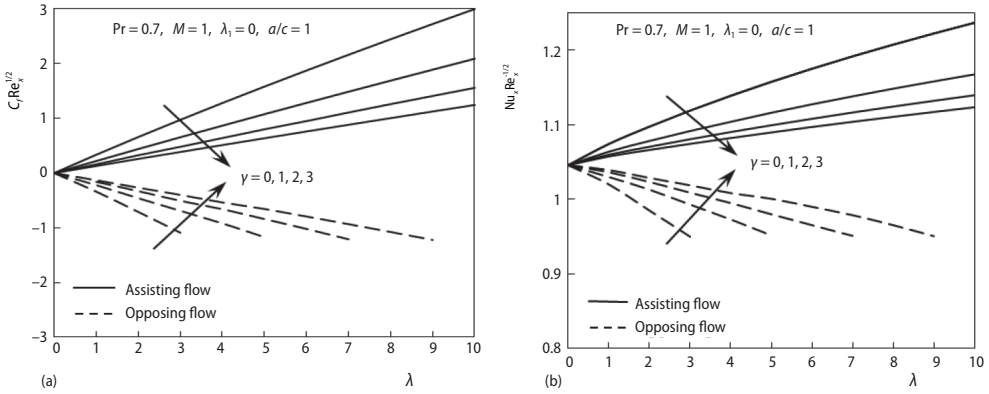

Figure 1. (a) skin friction coefficient and (b) local Nusselt number *vs.* λ for some values of γ when Pr = 0.7, $M = 1$, and $a/c = 1$

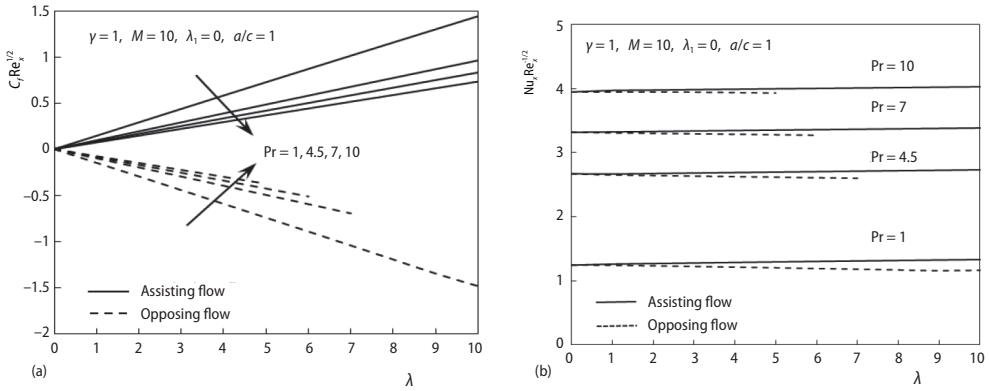

Figure 2. (a) skin friction coefficient and (b) local Nusselt number *vs.* λ for some values of Prandtl number when $\gamma = 1$, $M = 10$, and $a/c = 1$

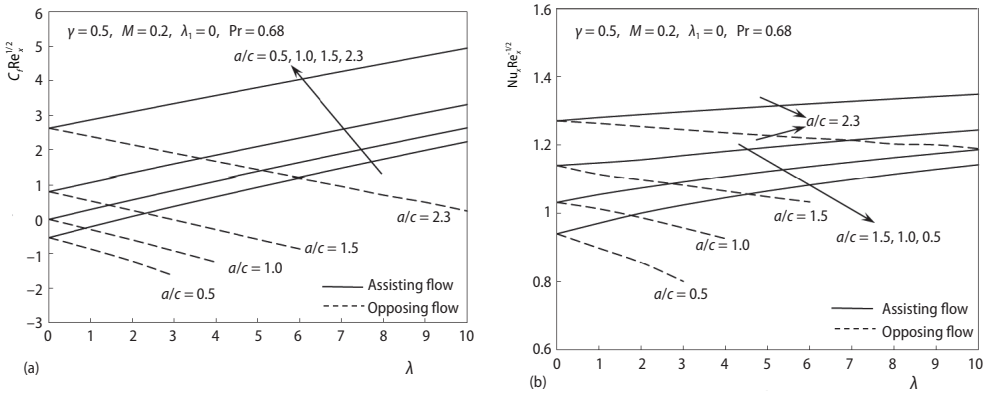

Figure 3. (a) skin friction coefficient and (b) local Nusselt number *vs.* λ for some values of a/c when $\gamma = 0.5$, $M = 0.2$, and Pr = 0.68

trated in fig. 1 when Pr = 0.7, $M = 1$, and $a/c = 1$. While the influence of the Prandtl number is depicted in fig. 2 for $\gamma = 1$, $M = 10$, and $a/c = 1$. Figure 3 shows the impact of a/c when $\gamma = 0.5$, $M = 0.2$, and Pr = 0.68. The profile of the dimensionless velocity $f'(\eta)$ and the dimensionless temperature $\theta(\eta)$ are depicted in figs. 4-7 for some values of the Deborah number, the Prandtl number, the mixed convection parameter, λ, and the velocity ratio, a/c, for both assisting and opposing flows, respectively.

Figures 1-3 suggest that for all positive values of the mixed convection parameter (assisting flow), the values of the skin friction coefficients and the local Nusselt numbers are found to exist, while there are restricted values of the skin friction coefficient and the local Nusselt number for the opposing flow. The assisting buoyant flow is found to increase the skin friction coefficient, while the opposing buoyant flow creates decrement of the skin friction coefficient as illustrated in figs. 1(a), 2(a), and 3(a). This is due to the assisting buoyant flow, which enhances the buoyancy force and hence, increases the fluid velocity. This action subsequently increases the wall shear stress, which increases the skin friction coefficient, Ishak *et al*. [4]. Referring to figs. 1(a) and 2(a), it should be noted that all curves intersect at a point when the buoyancy force is zero, $\lambda = 0$. In this case, $a/c = 1$ gives $C_f(\mathrm{Re}_x)^{1/2} = 0$. However, if $a/c \neq 1$, it should be expected that the intersection point is no longer fixed at 0, as $C_f(\mathrm{Re}_x)^{1/2}$ is very much influenced by the stretching velocity and the velocity of the external stream given by the constants a and c, respectively, as depicted in fig. 3(a). The figure also provides an idea of the point of intersection taking various values of a/c.

The effects of the material parameter γ on the skin friction coefficient and the local Nusselt number can be seen in figs. 1(a) and 1(b), when Pr = 0.7, $M = 1$, and $a/c = 1$ for both assisting and opposing flows. The values of $\mathrm{Nu}_x(\mathrm{Re}_x)^{-1/2}$ are found to coincide at 1.0458. The existence of the material parameter/Deborah number decreases the skin friction coefficient and surface heat transfer for the assisting flow. This is in line with the results obtained in tab. 2. Flow with a high Deborah number indicates that the fluid is dominated by elasticity, demonstrating solid-like behaviour, Reiner [34]. As such, the result is expected.

The effects of the Prandtl number on the skin friction coefficient and the local Nusselt number are depicted in figs. 2(a) and 2(b) when $\gamma = 1$, $M = 10$, and $a/c = 1$. It is seen that for a fixed value of λ, as Prandtl number increases, the value of the skin friction coefficient decreases and the local Nusselt number is found to increase for the assisting flow. Flow with a high value Prandtl number shows that the fluid is more viscous and, in return, retards the movement of the flow, hence reducing both the shear stress and the thermal conductivity on the surface. The implication can be seen in figs. 2(a) and 2(b), where the skin friction $C_f(\mathrm{Re}_x)^{1/2}$ decreases but the local Nusselt number $\mathrm{Nu}_x(\mathrm{Re}_x)^{-1/2}$ increases. The opposite trend occurs for the opposing flow. For a fixed value of Prandtl number, it is noted that the local Nusselt number slightly increases as the buoyant parameter λ is increased for assisting flow, as shown in fig. 2(b).

Figures 3(a) and 3(b) show the effect of a/c on the skin friction coefficient and the local Nusselt number when $\gamma = 0.5$, $M = 0.2$, and Pr = 0.68. It is noted that for the assisting flow, as λ increases, the skin friction coefficient and the local Nusselt number will increase, too. This is due to a large λ, which produces a large buoyancy force and in turn yields high kinetic energy to accelerate the fluid flow and increase the skin friction coefficient and the local Nusselt number. An increment of a/c will result in the increment of the skin friction coefficient and the local Nusselt number.

As prescribed in eq. (9), the velocity profiles $f'(\eta)$ in figs. 4(a), 5(a), and 6(a) begin at 1 at the beginning of the motion for both the assisting and opposing flows. For the assisting flow ($\lambda > 0$), the velocity increases slowly ($f' > 1$ in the boundary layer) until it achieved a cer-

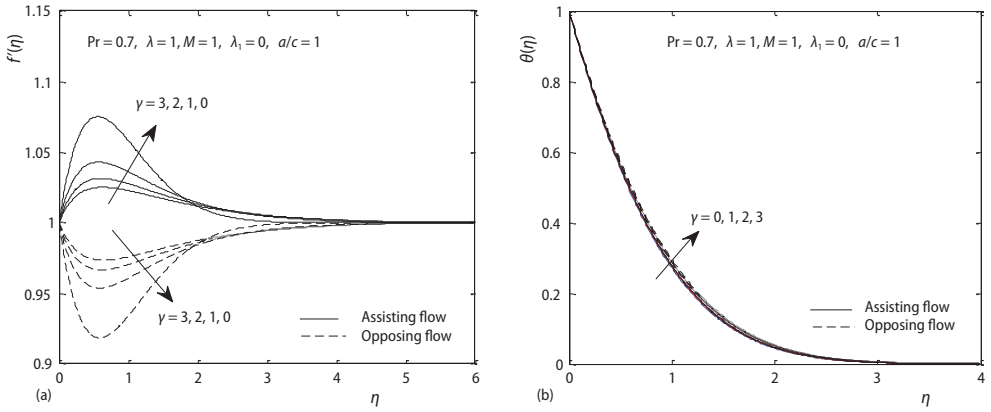

Figure 4. (a) velocity and (b) temperature profiles for some values of γ when $\lambda = 1$, Pr = 0.7, $M = 0.2$, and $a/c = 1$

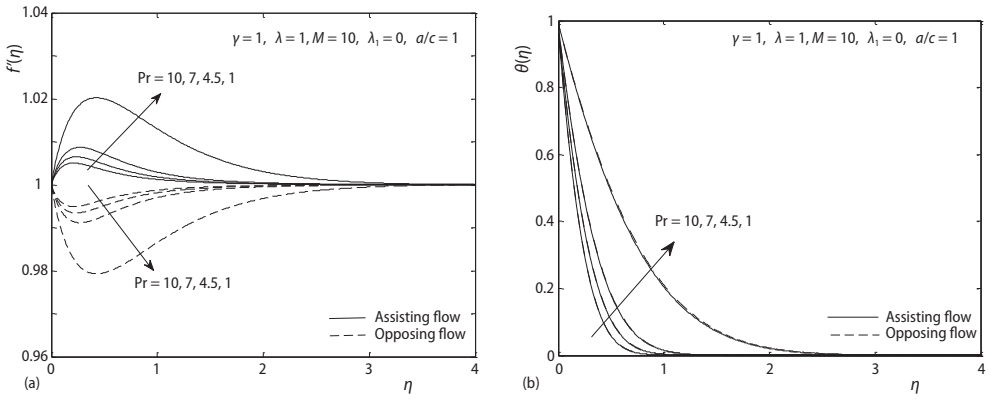

Figure 5. (a) velocity and (b) temperature profiles for some values of Prandtl number when $\gamma = 1$, λ=1, $M = 10$, and $a/c = 1$

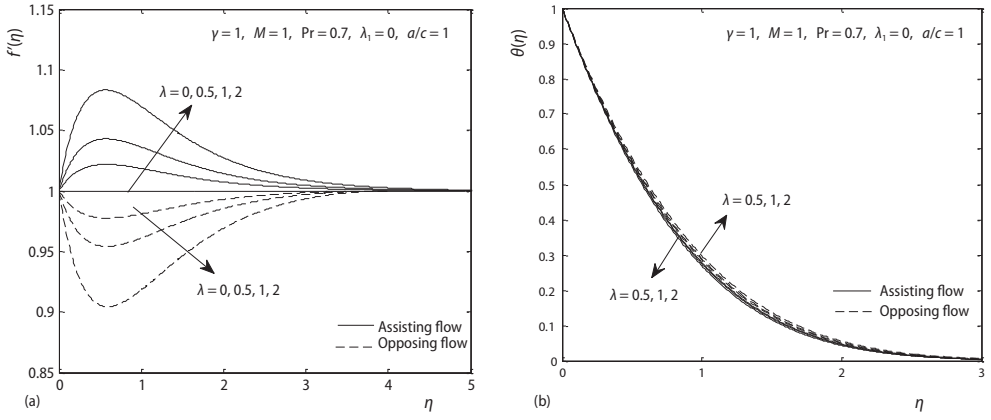

Figure 6. (a) velocity and (b) temperature profiles for some values of λ when $\gamma = 1$, $M = 1$, Pr = 0.7 and $a/c = 1$

tain value, then decreased asymptotically to a/c =1, (in this case) at the outside of the boundary layer. This is expected as the thermal expansion caused by the high wall temperature assists the flow. On the contrary, for the opposing flow, $f' < 1$ in the boundary layer due to the resistance of thermal expansion to the flow, Abbas *et al*. [16]. However, no boundary layer is formed when the buoyancy or mixed convection parameter is absent and the velocity $f' = 1$ throughout the flow domain, as illustrated in fig. 6(a).

Figure 4(a) shows that the magnitude of the velocity f' decreases with the increase of the Deborah number. As such, it may be expected that as $\gamma \to \infty$, $f' = 1$ in the whole flow domain. This is clear from the fact that γ measures the viscosity/elasticity of a fluid, as previously explained. The same phenomenon can be observed when $\mathrm{Pr} \to \infty$, as shown in fig. 5(a). Increasing the Prandtl number causes the decrease of the velocity flow and the temperature at the surface, as depicted in figs. 5(a) and 5(b). This is due to the fact that an increase in Prandtl number indicates the increase of the fluid heat capacity or the decrease of the thermal diffusivity, causing a diminution of the influence of the thermal expansion to the flow, Abbas *et al*. [16]. This results in faster formation of the thermal boundary layer and in turn, decreases the thermal boundary layer thickness as Prandtl number increases for both assisting and opposing flows.

The effect of the Deborah number and the mixed convection parameter are less pronounced with a variation in temperature, as can be seen in figs. 4(b) and 6(b). These figures clearly show that for the assisting flow, no temperature difference occurs for various values of γ and λ, while the temperature difference is conspicuous in the opposing flow. However, there is a slight difference in the temperature distribution for the opposing flow, *i. e.* at any point in the boundary layer, the temperature increases with the increase of γ, fig, 4(b) and λ, fig. 6(b), respectively. The thermal boundary layer thickness for both assisting and opposing flows are found to be more or less equal, as depicted in these two figures.

Figure 7(a) demonstrates the effect of a/c when $\lambda = 1$, $\mathrm{Pr} = 0.68$, $M = 0.2$, and $\gamma = 0.5$. It is noted that the flow, when the stretching velocity is less than the free stream velocity ($a/c > 1$), has a boundary layer structure and the thickness of the boundary layer decreases with an increase in a/c for both assisting and opposing flows. According to Mahapatra and Gupta [32], an increase in a in relation to c ($a/c > 1$) implies an increase in straining motion near the stagnation region, resulting in increased acceleration of the external stream, leading to increased velocity, which is then thinned by the boundary layer with an increase of a/c. This fact was experimentally confirmed by Flachsbart, Schlichting [35]. An inverted boundary layer is

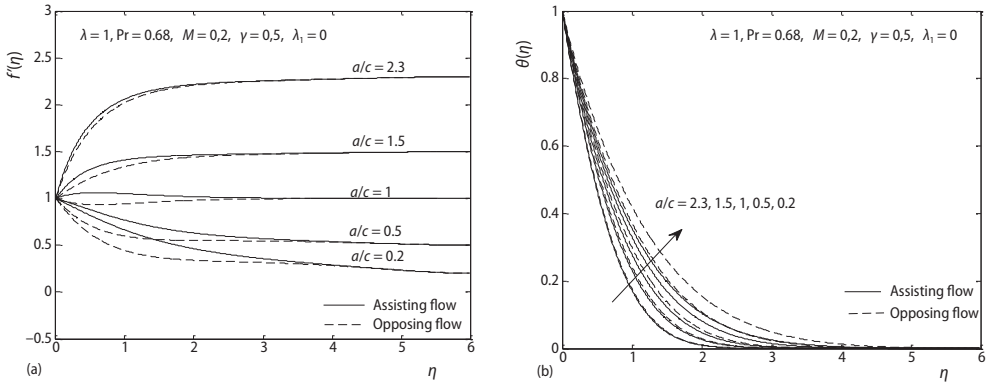

Figure 7. (a) velocity and (b) temperature profiles for some values of a/c when $\lambda = 1$, $\mathrm{Pr} = 0.68$, $M = 0.2$, and $\gamma = 0.5$

seen to form for $a/c < 1$ when the stretching velocity cx of the surface exceeds the velocity ax of the external stream. Figure 7(b) shows the temperature distribution in the thermal boundary layer. It is observed that the temperature of the fluid decreases as the distance from the surface is increased. The temperature at a point is found to decrease with the increase in a/c for both assisting and opposing flows. As such, flow with high a/c produces a thinner thermal boundary layer. The temperature for the opposing flow is slightly higher compared with the assisting flow at all points in the boundary layer, and the buoyancy effect is more pronounced for small a/c. Despite various profiles depicted in figs. 4-7, all the velocity and temperature profiles presented in those figures satisfy the far field boundary conditions (9) asymptotically, thus supporting the validity of the numerical results obtained.

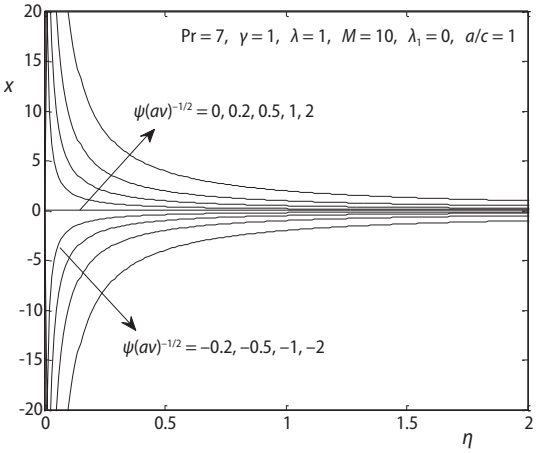

Figure 8. Streamlines for 2-D stretching sheet when Pr = 7, $\gamma = 1$, $\lambda = 1$, $M = 10$, and $a/c = 1$

Figure 8 shows the streamlines obtained for Pr = 7, $\gamma = 1$, $\lambda = 1$, $M = 10$, and $a/c = 1$ towards a stagnation point on a stretched vertical surface. The oncoming flow generated by the code is found to be satisfactory and hence we are confident of the results obtained in the present paper.

Conclusion

In this paper, the steady 2-D stagnation-point flow of a Jeffery fluid towards a vertical stretched surface in the presence of buoyancy force and magnetic field is investigated numerically using a finite difference scheme with an iterative technique. The problem is formulated in such a way that the stretching velocity and the surface temperature vary linearly with the distance from the stagnation point. The numerical solution obtained for the quantities of interest, which are the skin friction coefficient and the local Nusselt number for some values of the parameters, are displayed and discussed for both assisting and opposing flows. The flow with a high Deborah number is found to decrease the magnitude of the skin friction and the local Nusselt number for the assisting flow, while the opposite trend occurs for the opposing flow.

Nomenclature

a, b, c – constants, [–]
B_0 – uniform magnetic field, [T]
C_f – skin friction coefficient, [–]
f – dimensionless stream function, [–]
g – acceleration to gravity, [ms^{-1}]
Gr_x – local Grashof number, [–]
k – thermal conductivity, [Wm^{-1}K^{-1}]
M – magnetic parameter, [–]
Nu_x – local Nusselt number, [–]
Pr – Prandtl number, [–]
q_w – wall heat flux, [Wm^{-2}]
Re_x – local Reynolds number, [–]
T – fluid temperature, [K]
$T_w(x)$ – temperature of the stretching sheet, [K]
T_∞ – ambient temperature, [K]
u, v – velocity components along the x- and y-directions, respectively, [ms^{-1}]
u_e – velocity of the ambient fluid, [ms^{-1}]
x, y – Cartesian co-ordinates along the surface and normal to it, respectively,

Greek symbols

α – thermal diffusit, [m^{2}s^{-1}]
β – thermal expansion coefficient, [K^{-1}]
γ – Deborah number, [–]
η – similarity variable, [–]

θ – dimensionless parameter, [–]
λ – buoyancy or mixed convection parameter, [–]
λ_1 – ratio of the relaxation and retardation times, [–]
λ_2 – relaxation time, [s]
μ – dynamic viscosity, [$kgm^{-1}s^{-1}$]
ν – kinematic viscosity, [m^2s^{-1}]
ρ – fluid density, [kgm^{-3}]
σ – electrical conductivity, [Sm^{-1}]
τ_w – shear stress, [$kgm^{-1}s^{-2}$]
ψ – stream function, [–]

Subscripts

w – condition at the stretching sheet
∞ – condition at infinity

Superscript

$'$ – differentiation with respect to η

Acknowledgement

The first author gratefully acknowledge the financial support received in the form of a research grant (RAGS project code: RAGS13-003-0066) from the Ministry of Higher Education, Malaysia.

References

[1] Karwe, M. V., Jaluria, Y., Numerical Simulation of Thermal Transport Associated with a Continuously Moving Flat Sheet in Material Processing, *ASME Journal of Heat Transfer*, *113* (1991), 3, pp. 612-619
[2] Crane, L. J., Flow Past a Stretching Plate. *Zeitschrift für angewandte Mathematik und Physik ZAMP, 21* (1970), 4, pp. 645-647
[3] Hiemenz, K., The Boundary Layer Analysis of a Uniformly Flowing Liquid Circulating in Straight Circular Cylinder (in German), *Dinglers Polytechn. J, 326* (1911), pp. 321-324
[4] Ishak, A., *et al*., Mixed Convection Boundary Layers in the Stagnation-Point Flow toward a Stretching Vertical Sheet, *Meccanica*, *41* (2006), 5, pp. 509-518
[5] Ishak, A., *et al*., Unsteady Mixed Convection Boundary Layer Flow due to a Stretching Vertical Surface, *Arabian Journal for Science and Engineering, 31* (2006), 2B, pp. 165-182
[6] Ishak, A., *et al*., MHD Mixed Convection Boundary Layer Flow towards a Stretching Vertical Surface with Constant Wall Temperature, *International Journal of Heat and Mass Transfer, 53* (2010), 23-24, pp. 5330-5334
[7] Pal, D., Heat and Mass Transfer in Stagnation-Point Flow towards a Stretching Surface in the Presence of Buoyant Force and Thermal Radiation, *Meccanica*, *44* (2009), 2, pp. 145-158
[8] Ali, F. M., *et al*., MHD Mixed Convection Boundary Layer Flow toward a Stagnation Point on a Vertical Surface with Induced Magnetic Field, ASME *Journal of Heat Transfer, 133* (2010), 2, pp. 022502-022507
[9] Chen, C. H., Mixed Convection Unsteady Stagnation-Point Flow towards a Stretching Sheet with Slip Effects, *Mathematical Problems in Engineering*, *2014* (2014), ID 435697
[10] Saleh, S. H. M., *et al.,* Mixed Convection Stagnation-Flow towards a Vertical Shrinking Sheet, *International Journal of Heat and Mass Transfer, 73* (2014), June, pp. 839-848
[11] Ellahi, R., *et al*., A Study on the Mixed Convection Boundary Layer Flow and Heat Transfer over a Vertical Slender Cylinder*, Thermal Science, 18* (2014), 4, pp. 1247-1258
[12] Rashidi, M. M., Mehr, N. F., Series Solutions for the Flow in the Vicinity of the Equator of an Magnetohydrodynamic Boundary-Layer over a Porous Rotating Sphere with Heat Transfer, *Thermal Science, 18* (2014), Suppl. 2, pp. S527-S537
[13] Rashidi, S., *et al*. Study of Stream Wise Transverse Magnetic Fluid Flow with Heat Transfer around a Porous Obstacle, *Journal of Magnetism and Magnetic Materials, 378* (2015), Mar., pp. 128-137
[14] Boričić, A. Z., *et al*., Magnetohydrodynamic Effects on Unsteady Dynamic, Thermal and Diffusion Boundary Layer Flow over a Horizontal Circular Cylinder, *Thermal Science, 16* (2012), Suppl. 2, pp. S311-S321
[15] Lok, Y., *et al.,* Unsteady Mixed Convection Flow of a Micropolar Fluid Near the Stagnation- Point on a Vertical Surface, *International Journal of Thermal Sciences, 45* (2006), 12, pp. 1149-1157

[16] Abbas, Z., *et al.,* Mixed Convection in the Stagnation-Point Flow of a Maxwell Fluid towards a Vertical Stretching Surface, *Nonlinear Analysis: Real World Applications, 11* (2010), 4, pp. 3218-3228
[17] Ahmad, K., Nazar, R., Unsteady Magnetohydrodynamic Mixed Convection Stagnation-Point Flow of a Viscoelastic Fluid on a Vertical Surface, *Journal of Quality Measurement and Analysis, 6* (2010), 2, pp. 105-117
[18] Das, K., Slip Effects on MHD Mixed Convection Stagnation-Point Flow of a Micropolar Fluid towards a Shrinking Vertical Sheet, *Computers & Mathematics with Applications, 63* (2012), 1, pp. 255-267
[19] Makinde, O. D., *et al*., Buoyancy Effects on MHD Stagnation-Point Flow and Heat Transfer of a Nanofluid Past a Convectively Heated Stretching/Shrinking Sheet, *International Journal of Heat and Mass Transfer, 62* (2013), July, pp. 526-533
[20] Ellahi, R., The Effects of MHD and Temperature Dependent Viscosity on the Flow of Non-Newtonian Nanofluid in a Pipe: Analytical Solutions, *Applied Mathematical Modelling, 37* (2013), 3, pp. 1451-1457
[21] Ellahi, R., *et al*., M., Series Solutions of Magnetohydrodynamic Peristaltic Flow of a Jeffrey Fluid in Eccentric Cylinders, *Applied Mathematics & Information Sciences, 7* (2013), 4, pp. 1441-1449
[22] Singh, V., Agarwal, S., MHD Flow and Heat Transfer for Maxwell Fluid over an Exponentially Stretching Sheet with Variable Thermal Conductivity in Porous Medium, *Thermal Science, 18* (2014), Suppl. 2, pp. S599-S615
[23] Abdel-Rahman, G. M., Effects of Variable Viscosity and Thermal Conductivity on Unsteady MHD Flow of Non-Newtonian Fluid over a Stretching Porous Sheet, *Thermal Science, 17* (2013), 4, pp. 1035-1047
[24] Yacob, N. A. *et al*., Hydromagnetic Flow and Heat Transfer Adjacent to a Stretching Vertical Sheet in a Micropolar Fluid, *Thermal Science, 17* (2013), 2, pp. 525-532
[25] Sheikholeslami, M., *et al.,* Effects of MHD on Cu-Water Nanofluid Flow and Heat Transfer by Means of CVFEM, *Journal of Magnetism and Magnetic Materials*, *349* (2014), Jan., pp. 188-200
[26] Zeeshan, A., *et al*., Magnetohydrodynamic Flow of Water/Ethylene Glycol Based Nanofluids with Natural Convection Through Porous Medium, *The European Physical Journal Plus*, *129* (2014), Dec., pp. 261-270
[27] Lin, Y., *et al*. MHD Thin Film and Heat Transfer of Power Law Fluids over an Unsteady Stretching Sheet with Variable Thermal Conductivity, *Thermal Science, 20* (2015), 6, pp. 1791-1800
[28] Hayat, T., *et al*., An Analysis of Peristaltic Transport for Flow of a Jeffrey Fluid, *Acta Mechanica, 193* (2007), 1-2, pp. 101-112
[29] Ramachandran, N., *et al.,* Mixed Convection in Stagnation Flows Adjacent to Vertical Surfaces, *ASME Journal of Heat Transfer, 110* (1988), 2, pp. 373-377
[30] Cebeci, T., *Convective Heat Transfer*, Horizon Publishing, Bishop, Cal., USA, 2002
[31] Cebeci, T., Bradshaw, P., *Physical and Computational Aspects of Convective Heat Transfer*, Springer, New York, USA, 1988
[32] Mahapatra, T. R., Gupta, A. S., Heat Transfer in Stagnation-Point Towards a Stretching Sheet, *Heat Mass Transfer, 38* (2002), 6, pp. 517-521
[33] Nazar, R., *et al*., Unsteady Boundary Layer Flow in the Region of the Stagnation Point on a Stretching Sheet, *International Journal of Engineering Science, 42* (2004), 11-12, pp. 1241-1253
[34] Reiner, M., The Deborah Number, *Physics Today*, *17* (1964), 1, p. 62
[35] Schlichting, H., *Boundary Layer Theory*, McGraw-Hill, New York, USA, 1968

Paper submitted: November 3, 2014
Paper revised: February 10, 2015
Paper accepted: February 24, 2015